

Isotropic–nematic phase transition in the Lebwohl–Lasher model from density of states simulations

Raj Shekhar, Jonathan K. Whitmer, Rohit Malshe, J. A. Moreno-Razo, Tyler F. Roberts et al.

Citation: *J. Chem. Phys.* **136**, 234503 (2012); doi: 10.1063/1.4722209

View online: <http://dx.doi.org/10.1063/1.4722209>

View Table of Contents: <http://jcp.aip.org/resource/1/JCPSA6/v136/i23>

Published by the [American Institute of Physics](#).

Additional information on J. Chem. Phys.

Journal Homepage: <http://jcp.aip.org/>

Journal Information: http://jcp.aip.org/about/about_the_journal

Top downloads: http://jcp.aip.org/features/most_downloaded

Information for Authors: <http://jcp.aip.org/authors>

ADVERTISEMENT



ACCELERATE AMBER AND NAMD BY 5X.
TRY IT ON A FREE, REMOTELY-HOSTED CLUSTER.

[LEARN MORE](#)

Isotropic–nematic phase transition in the Lebwohl–Lasher model from density of states simulations

Raj Shekhar,¹ Jonathan K. Whitmer,¹ Rohit Malshe,¹ J. A. Moreno-Razo,²
Tyler F. Roberts,¹ and Juan J. de Pablo^{1,a)}

¹*Department of Chemical and Biological Engineering, University of Wisconsin, Madison, Wisconsin 53706-1691, USA*

²*Departamento de Física, Universidad Autónoma Metropolitana-Iztapalapa, Apartado Postal 55-534, México 09340, Distrito Federal, México*

(Received 22 February 2012; accepted 11 May 2012; published online 19 June 2012)

Density of states Monte Carlo simulations have been performed to study the isotropic–nematic (IN) transition of the Lebwohl–Lasher model for liquid crystals. The IN transition temperature was calculated as a function of system size using expanded ensemble density of states simulations with histogram reweighting. The IN temperature for infinite system size was obtained by extrapolation of three independent measures. A subsequent analysis of the kinetics in the model showed that the transition occurs via spinodal decomposition through aggregation of clusters of liquid crystal molecules.

© 2012 American Institute of Physics. [<http://dx.doi.org/10.1063/1.4722209>]

I. INTRODUCTION

Liquid crystals (LCs) are materials which simultaneously exhibit the order found in solids and the fluidity of liquids. These materials can exhibit transitions between multiple phases. Two commonly studied LC phases are the isotropic and nematic phases. The isotropic phase exhibits no translational or orientational order, while the nematic phase exhibits short-range orientational order. The nature of the isotropic–nematic (IN) phase transition is relevant for many technological applications.

Beyond having a rich phase behavior, LC systems exhibit interesting dynamic properties.^{1,2} An important question is whether the phase transition occurs via spinodal decomposition or via nucleation and growth. In the spinodal decomposition, LC molecules associate together to form clusters. These clusters are formed randomly, and molecules can move in or out of them. Near the phase transition, the distribution of cluster sizes is not correlated with the overall order parameter. The phenomenon of nucleation and growth involves the formation of one or more ordered domains, which will grow or decay. Domains exceeding a critical size continue to grow until the system ultimately adopts an overall ordered structure. Previous computational studies of LC models have examined both mechanisms.^{1,3–15} Here, we examine the nature of the IN phase transition using the Lebwohl–Lasher (LL) model, a minimal lattice LC model whose simplicity has attracted significant research.^{4,7,13,14,16–22} To the best of our knowledge, the transition mechanism for the LL model has not been studied previously. To do this, we adapt a novel approach for the identification of ordered domains originally proposed in the context of colloidal hard rods by Cuetos and Dijkstra.⁵

The paper is organized as follows. In Sec. II, we describe the LL model. Section III contains an overview of the expanded ensemble density of states (EXEDOS) algorithm

and histogram reweighting techniques employed in this work. Section IV describes the clustering criteria used to distinguish isotropic and nematic domains, and their application to the study of kinetic pathways relevant to the IN transition. In Sec. V we present the results of our simulations and provide a general discussion of our findings.

II. LEBWOHL–LASHER (LL) MODEL

The LL model²³ is a lattice version of the Maier–Saupe model²⁴ for anisotropic liquid crystalline materials. Mesogens are represented by “spins” (unit vectors) placed on the nodes of a cubic lattice with periodic boundaries.²⁵ These spins interact through a Hamiltonian given by

$$H = -\epsilon \sum_{i,j} P_2(\cos \theta_{ij}), \quad (1)$$

where $P_2(z) = \frac{1}{2}(3z^2 - 1)$ is the second Legendre polynomial, θ_{ij} is the angle between the unit vectors associated with nearest-neighbor spins, and ϵ is an energy parameter that measures the interaction strength between neighboring mesogens. Setting this parameter to unity defines the natural unitless temperature for the system as kT/ϵ . From here, we will assume reduced units and simply write the temperature as T , with potential and free energies similarly normalized.

While the LL model neglects interactions between translational and orientational degrees of freedom, this attractive simplicity has spawned extensive study.^{4,7,13,14,16–22} Zhang *et al.* (see Ref. 26) used Monte Carlo simulations for systems of different sizes and found that the isotropic nematic transition temperature occurs at $T_{\text{IN}} = 1.1232 \pm 0.0001$. A subsequent study by Priezjev and Pelcovits¹⁸ of larger lattices, utilizing a cluster Monte Carlo approach yielded a lower transition temperature, $T_{\text{IN}} = 1.1225 \pm 0.0001$. To address this discrepancy, and to inform our kinetic studies, we examine this transition using density of states (DOS) based

^{a)}Electronic mail: depablo@engr.wisc.edu.

simulations. DOS studies have previously been carried out using histogram reweighting and finite-size scaling techniques.^{3,26} Most studies have concluded that the LL model exhibits a weak first order isotropic–nematic phase transition.^{26,27}

Our simulations utilize periodic boundary conditions in all directions. Simulations are performed at various temperatures and system sizes (determined by $N = L^3$, where L is the number of lattice nodes in each direction). Further relevant details follow in Sec. V.

III. EXEDOS ALGORITHM

The expanded ensemble density of states (EXEDOS) method is a variant of Wang–Landau sampling,^{28,29} which allows direct determination of the free energy with respect to a convenient order parameter or reaction coordinate.³⁰ For a phase transition study, the order parameter should clearly distinguish the coexisting phases near the boundary of interest.

The structure of LC systems is readily quantified by the tensor order parameter \mathbf{Q} . The scalar order parameter $S \in [-\frac{1}{2}, 1]$ represents the maximum positive eigenvalue of \mathbf{Q} . The corresponding eigenvector is parallel to the nematic director. The tensor may be calculated via

$$Q_{\alpha\beta} = \frac{1}{2N} \sum_{i=1}^N [3u_{i\alpha}u_{i\beta} - \delta_{\alpha\beta}], \quad (2)$$

where, $u_{i\alpha}$ is the α component of the i th spin orientation \mathbf{u}_i . The remaining terms include the Kronecker delta $\delta_{\alpha\beta}$, and N , the total number of spins. S assumes a value close to zero in the isotropic phase, and a value in the range 0.4–0.8 for nematic phases.³¹

Our implementation of EXEDOS is described below. For a more complete description of EXEDOS and similar algorithms, readers are referred to Refs. 28, 30, 32–34. The density of states at a given inverse temperature $\beta = 1/k_B T$ and order parameter S is denoted by $\Omega(S, \beta)$. We note that $\Omega(S, \beta)$ relates to the Landau free energy of a state S via

$$\Omega(S, \beta) \propto \omega(S, \beta) = e^{-\beta F(S)}, \quad (3)$$

where $\omega(S, \beta)$ is the normalized probability distribution of states S . EXEDOS derives its name from the expansion of the ensemble to include the order parameter S as a thermodynamic variable. The algorithm proceeds through the partitioning of phase space into bins along the order parameter, with subsequent evolution of the system by MC moves in the standard ensemble (e.g., NVT) modified by an accumulated bias against previously visited states. Each bin S is assigned a histogram entry and a statistical weight $\tilde{\Omega}(S)$, an estimator for $\Omega(S, \beta)$, which are evolved in the following way. Each visit to the state S increments the histogram by one, and modifies the estimator by a convergence factor f , $\tilde{\Omega}(S) \rightarrow f\tilde{\Omega}(S)$. This is equivalent to the addition of a bias energy $\log f$ against the state S . The estimator is used to bias the acceptance of future moves according to

$$\text{Acc}(\text{old} \rightarrow \text{new}) = \min \left\{ 1, \frac{\tilde{\Omega}_{\text{old}}}{\tilde{\Omega}_{\text{new}}} \exp[-\beta(U_{\text{new}} - U_{\text{old}})] \right\}. \quad (4)$$

Simulations are evolved until the histogram becomes sufficiently flat, at which point it is zeroed and the convergence factor is updated according to $f_{\text{new}} = f_{\text{old}}^{1/2}$. As $\log f \rightarrow 0$, detailed balance is satisfied²⁸ and $\tilde{\Omega}(S) \rightarrow \Omega(S, \beta)$. We note that bins must be small enough to promote evolution of the system along the order parameter and expedite convergence. The meaning of the Landau free energy associated with a converged probability distribution $\omega(S, \beta)$ depends on the original simulation ensemble. Our simulations here are based on constant- NVT conditions, thus the resulting quantity is the Helmholtz free energy.

Away from T_{IN} , $F(S, \beta)$ exhibits a single minimum. Near the transition temperature, it is expected to develop two minima, with the barrier between them corresponding to the formation of an interface. Since the transition temperature is not known *a priori*, a series of simulations are carried out at different temperatures. At the transition temperature, the free energy exhibits two equal-depth minima. The process of identifying T_{IN} for a given system size L may be facilitated considerably through the use of histogram reweighting.³⁵ In this approach, energy data from EXEDOS simulations are recorded for each order parameter bin. The probability distribution $\omega(S, \beta_2)$ may then be obtained from simulations performed at inverse temperature β_1 as

$$\omega(S, \beta_2) = \frac{\omega(S, \beta_1) \sum_{i=1}^{N_S} \exp((\beta_1 - \beta_2)U_{S,i})}{\sum_{S=S_{\text{low}}}^{S_{\text{high}}} \omega(S, \beta_1) \sum_{i=1}^{N_S} \exp((\beta_1 - \beta_2)U_{S,i})}, \quad (5)$$

where $U_{S,i}$ and N_S are the energy stored in bin i and the number of histogram entries corresponding to a value of the order parameter S . The order parameter range is bounded by S_{low} and S_{high} .

It should be noted that the chief benefit in using EXEDOS over conventional Monte Carlo sampling methods is that a converged EXEDOS simulation obtains the *exact* free energy surface as a function of the order parameter(s) by construction. By contrast, other methods will be limited in their sampling capability, since their error will strongly depend on the depth of free energy basins, and the height of barriers separating the two states. While it should be expected that other sampling methods can approach the true free energy surface given sufficient simulation length, the degree of convergence to the free energy surface is still an unknown quantity. This is particularly important to histogram reweighting schemes, since EXEDOS ensures that rarely sampled states are accurately weighted initially, limiting the propagation of error in histogram reweighting. We therefore expect more accurate results to be obtained from this method relative to simulations which sample the NVT ensemble alone (e.g., Ref 18).

IV. STUDY OF KINETIC PATHWAYS OF IN TRANSITION

To study the kinetic pathways for the IN transition using Monte Carlo (MC) simulations, it is necessary to devise a scheme that can distinguish nematic clusters from isotropic domains. In their work on colloidal hard rods, Cuetos and Dijkstra⁵ used a novel cluster criterion to identify nematic clusters. In this work, we follow their approach, which involves two steps. In the first, a nematic-like particle is

identified. A particle is considered nematic-like if its local environment exhibits an orientational order parameter value that is significantly higher than that of the isotropic phase. The local environment of particle i is defined through the orientation of all neighbors located within two lattice units. The order parameter for the local environment associated with particle i is defined by

$$S(i) = \frac{1}{n_i} \sum_{j=1}^{n_i} \left(\frac{3}{2} |\mathbf{u}_j \cdot \mathbf{u}_i|^2 - \frac{1}{2} \right), \quad (6)$$

where n_i is the number of neighbors of i used to specify its local environment. Particle i is considered to be nematic-like if $S(i) > 0.4$. The second step involves recursively merging these nematic-like particles to identify nematic clusters. Particles i and j belong to the same cluster if they are located at a distance equivalent to a lattice unit and have a dot product of associated spins $|\mathbf{u}_j \cdot \mathbf{u}_i| > 0.85$. This cluster criterion can be used to identify the largest nematic cluster present in the system.

To study the kinetic pathways for the IN transition, MC simulations well inside the nematic phase can be performed starting from an initial isotropic state. As the system is evolved, a transition from the isotropic to the nematic phase occurs. We record the order parameter and size of the largest nematic cluster periodically. The order parameter generally increases with the number of simulation steps almost monotonically, and attains a particular equilibrium value after a few steps. If the curve representing the time evolution of the largest cluster shows a monotonic increase, then the system can be considered to exhibit the characteristics of nucleation and growth. In that case, the order-parameter curve lags behind the curve representing the size of the largest nematic cluster when plotted against the number of MC cycles. If, on the other hand, the curve representing the largest cluster size lags behind the order parameter curve, the system is considered to undergo a phase transition via spinodal decomposition.

V. RESULTS

A. Isotropic–nematic transition temperature

Data were collected for systems of size $N = \{10^3, 12^3, 15^3, 20^3, 25^3, 30^3, 35^3, 40^3\}$ at the same reduced temperature $T = 1.125$, identified on the basis of initial exploratory simulations.

Figure 1 shows the free energy as a function of order parameter for systems of different sizes, improving upon previously reported results.²⁶ These free energy profiles were generated directly from EXEDOS simulations without histogram reweighting, and demonstrate clearly the dramatic finite size effects present in the model. The location of a minimum in S determines the isotropic or nematic state. At this temperature, the smallest system (10^3) is in the nematic phase, whereas the largest system (40^3) is well in the isotropic phase.

A finite-size scaling procedure is performed to determine the transition temperature corresponding to an infinite system. Histogram reweighting was used to generate free energy profiles for each system size at several temperatures. For each

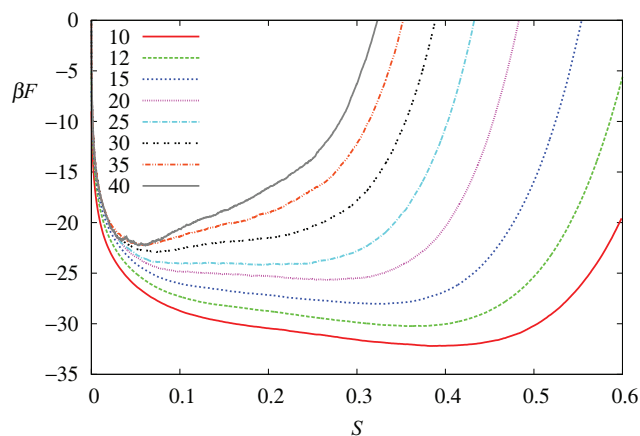


FIG. 1. Free energy profile as a function of order parameter for the Lebwohl–Lasher model from the simulations of different lattice sizes. The results serve to illustrate the existence of pronounced finite-size effects, and indicate that the accurate determination of thermodynamic properties requires that large systems be considered.

system size, the temperatures at which the two minima had equal depth were identified with the IN transition. Figure 2 shows the free energy profile for the five largest systems at their value of T_{IN} , identified via the criterion of equal depth in the free energy profile. The transition temperature calculated from each exhibits a linear trend in L^{-3} for our five largest systems.

The temperature at which the free energy profile shows two identical minima, which correspond to the isotropic and nematic phases, is the transition temperature for that particular system size. The transition temperature for $L = 40$ is $T_{IN} = 1.1232$. Using the same approach, the IN transition temperature was obtained for systems of different size.

Following the approach of Lee and Kosterlitz³⁶ (LK), T_{IN} obtained from the equal-depth free energy curve was plotted against the inverse of the corresponding lattice size. In

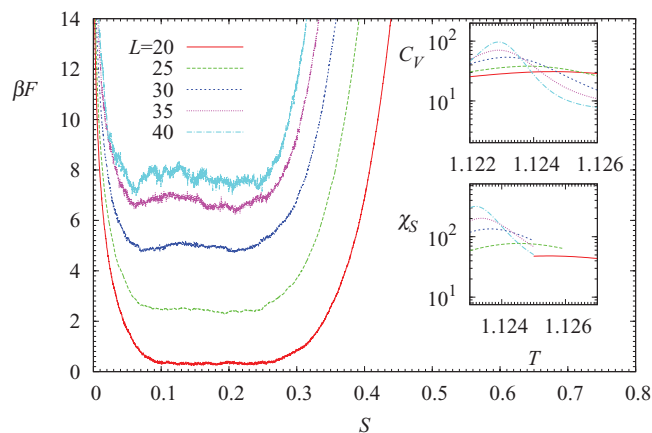


FIG. 2. (Main) Free energy profiles for the five largest system sizes examined here, obtained through the histogram reweighting of individual EXEDOS simulations at $T = 1.125$. Graphs have been displaced along the free energy axis for clarity. (Upper inset) Specific heat of each system as a function of temperature, with the trends of decreasing peak temperature and increasing divergence in the heat capacity clearly visible. (Lower inset) Same as previous, plotting nematic susceptibility (χ_S) instead of specific heat.

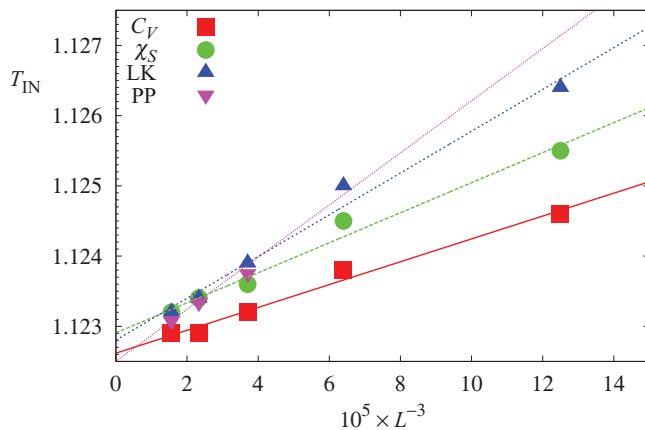


FIG. 3. Finite size scaling of the IN transition temperature. Solid and dashed lines indicate best fit to the data of the same color. Data plotted are for T_{IN} determined via specific heat (C_V), via nematic susceptibility (χ_S), and via the method of Lee and Kosterlitz (LK).³⁶ For comparison, data from the paper of Priezjev and Pelcovits (PP)¹⁸ are also shown, along with the line of best fit from Ref. 18.

this scaling, the results obtained from small systems were left out, owing to significant deviations from the linear trend observed for the larger systems. From the intercept of the linear fit (cf. Fig. 3) with the temperature axis, the transition temperature in the limit of infinite size was determined to be $T_{\text{IN}}^{LK} = 1.1229 \pm 0.00015$. This value is in close agreement with that estimated by Zhang *et al.*,²⁶ who proposed $T_{\text{IN}} = 1.1232 \pm 0.0001$. Note that Zhang *et al.* considered systems of sizes up to 28^3 . These data also agree favorably with the transition temperature obtained from larger systems by Priezjev and Pelcovits (PP),³⁶ who obtained a transition temperature $T_{\text{IN}} = 1.1225 \pm 0.0001$. We note that the direct comparison of overlapping data points ($L = \{30, 35, 40\}$) plotted in Figure 3 shows that PP underestimate the transition temperature of these systems compared to the values obtained by reweighting of the converged density of states.

Alternate measures for the transition temperature may be obtained from peaks in the specific heat

$$C_V = \frac{\beta^2}{L^3} (\langle U^2 \rangle - \langle U \rangle^2), \quad (7)$$

and nematic susceptibility

$$\chi_S = L^3 (\langle S^2 \rangle - \langle S \rangle^2), \quad (8)$$

when plotted versus T . The corresponding curves are provided in the insets to Figure 2. These other measures yield results consistent with those obtained from EXEDOS, $T_{\text{IN}}^{C_V} = 1.1226 \pm 0.0001$ and $T_{\text{IN}}^{\chi_S} = 1.1228 \pm 0.00014$.

B. Kinetic pathways for IN transition

Having identified the precise location of the IN transition temperature, we proceed to examine the kinetic pathways for that transition. To that end, simulations were performed for a system of size 30^3 at a reduced temperature of 0.70. At this temperature, starting from an isotropic initial configuration (with the orientation of spins randomly assigned), the sys-

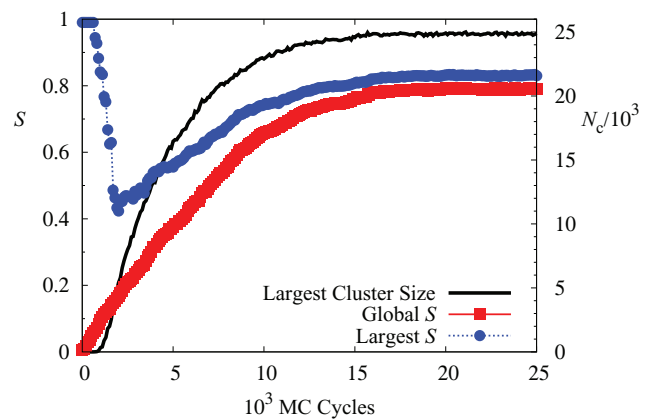


FIG. 4. (Black curve) Evolution of size and nematic order parameter of the largest cluster in the Lebwohl-Lasher system. N_c refers to the number of spins in the largest cluster. The nematic order parameter of the largest cluster (blue curve) has been compared against the global nematic order parameter (red curve). The drop in order parameter of the largest cluster leads to our view that the phase transition occurs through a spinodal decomposition mechanism.

tem undergoes a transition from isotropic to nematic. Figure 4 shows the evolution of the largest nematic cluster as the simulation progresses. It also shows the nematic order parameter of the largest cluster as well as the global nematic order parameter of the system, both as a function of time (MC cycles). All spins in the system are moved once during an individual MC cycle.

At the beginning of the simulation, nematic clusters are small in size, with the largest cluster consisting of only a few hundred spins. These clusters are highly ordered, and have a nematic order parameter close to 0.9. As the simulation progresses, neighboring clusters merge together to form larger clusters. As the size of the largest cluster increases, its overall order shows a sharp decline owing to the fact that different merging clusters exhibit different orientations. As the system is allowed to equilibrate in the nematic state, the nematic order, as well as the number of particles associated with the largest cluster, grow monotonically until the largest cluster is comparable to the size of the system. This behavior is typical of spinodal decomposition.³⁷

Figure 5 provides snapshots of the largest nematic cluster along with the order parameter map of the system at different time points. Local order maps are shown for the sections passing through the center of the largest cluster along three perpendicular planes. We observe isolated clusters in the early stages of the simulation. These clusters become prominent after 1000 MC cycles. After 2000 MC cycles, these clusters merge with each other to form a much larger cluster, with low nematic order. This corresponds to the minimum point in the local order profile of the largest cluster in Figure 4. At this point, the largest cluster consists of several regions with varying orientations. As the simulation progresses, after 3000 MC cycles, the largest cluster grows in size along with increasing local order. We also show the late stages of the system when it has reached the fully nematic state, after 20 000 MC cycles. At this point, there is a single nematic cluster that spans the entire system.

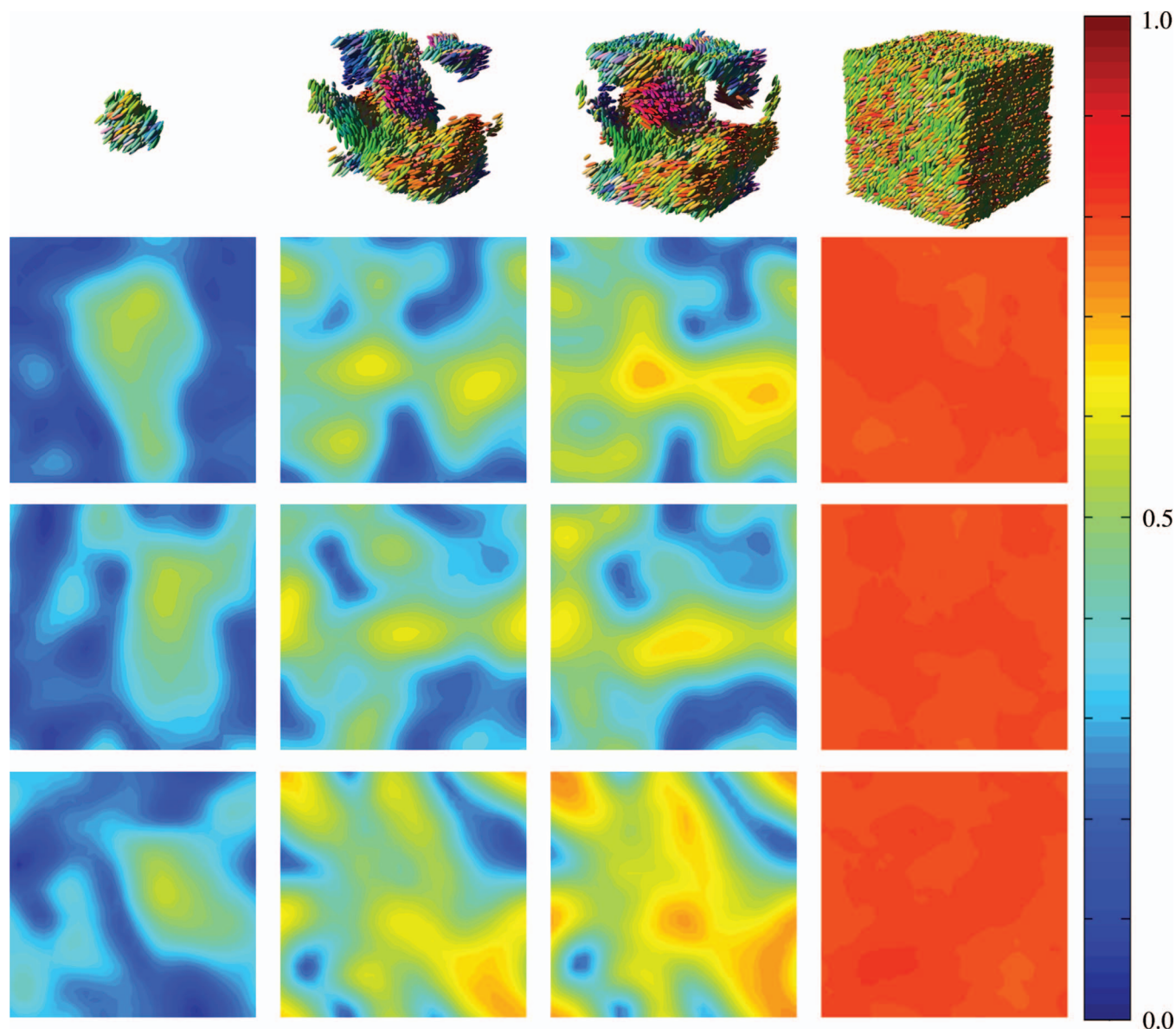


FIG. 5. Evolution of the largest nematic cluster and local order parameter map. The columns (from left to right) provide representative configurations extracted from a simulation after 1000, 2000, 3000, and 20 000 MC cycles. The rows (top to bottom) show snapshots of the largest clusters and the global nematic order map in cross-sections that pass through the center of the largest cluster and are perpendicular to the X (second row), Y (third row), and Z (fourth row) axes. Maps are colored according to the scale (blue to red) at right. The colors of the spins in the cluster represent their orientation with red-green-blue corresponding to direction vectors according to $[R, G, B]$.

VI. CONCLUSIONS

Density of states simulations of the IN transition in the LL model have been used to provide an accurate estimate of the transition temperature. The systems considered in this work were studied via the EXEDOS method, which allows the exact determination of the free energy surface. From these converged profiles, the size dependent transition temperatures was accurately determined and extrapolated to the thermodynamic limit. Further, we have shown this measure to be completely consistent with other thermodynamic measures; as such, the transition temperature put forth in this work should be viewed as the most reliable estimate to date. For a large system size, a subsequent analysis of the kinetics of the phase transition after a deep quench from the isotropic to the ne-

matic phase indicated that the transition occurs through spinodal decomposition.

ACKNOWLEDGMENTS

This work is supported by the Department of Energy, Basic Energy Sciences, Biomaterials Program (DE-SC0004025).

¹N. S. Skantzos and J. P. L. Hatchett, *Physica A* **381**, 202 (2007).

²M. P. Allen and M. A. Warren, *Phys. Rev. Lett.* **78**, 1291 (1997).

³K. Mukhopadhyay, N. Ghoshal, and S. K. Roy, *Phys. Lett. A* **372**, 3369 (2008).

⁴H. Chamati and S. Romano, *Phys. Rev. E* **77**, 051704 (2008).

⁵A. Cuetos and M. Dijkstra, *Phys. Rev. Lett.* **98**, 095701 (2007).

⁶G. Celebre and G. Cinacchi, *Phys. Rev. E* **73**, 020702 (2006).

- ⁷S. Chakrabarty, D. Chakrabarti, and B. Bagchi, *Phys. Rev. E* **73**, 061706 (2006).
- ⁸M. Krasna, R. Repnik, Z. Bradac, and S. Kralj, *Mol. Cryst. Liq. Cryst.* **449**, 127 (2006).
- ⁹E. Lomba, C. Martin, N. G. Almarza, and F. Lado, *Phys. Rev. E* **74**, 021503 (2006).
- ¹⁰M. P. Allen, *Phys. Rev. E* **72**, 036703 (2005).
- ¹¹I. Amimori, J. N. Eakin, J. Qi, G. Skacej, S. I. Zumer, and G. P. Crawford, *Phys. Rev. E* **71**, 031702 (2005).
- ¹²C. Chiccoli, P. Pasini, G. Skacej, and C. Zannoni, *Mol. Cryst. Liq. Cryst.* **429**, 255 (2005).
- ¹³D. Jayasri, V. S. S. Sastry, and K. P. N. Murthy, *Phys. Rev. E* **72**, 036702 (2005).
- ¹⁴E. Mondal and S. K. Roy, *Phys. Lett. A* **324**, 337 (2004).
- ¹⁵M. Svetec, Z. Bradac, S. Kralj, and S. Zumer, *Mol. Cryst. Liq. Cryst.* **413**, 2179 (2004).
- ¹⁶S. Dutta and S. K. Roy, *Phys. Rev. E* **70**, 066125 (2004).
- ¹⁷S. Romano, *Physica A* **322**, 432 (2003).
- ¹⁸N. V. Priezjev and R. A. Pelcovits, *Phys. Rev. E* **63**, 062702 (2001).
- ¹⁹S. J. Mills and D. J. Cleaver, *Mol. Phys.* **98**, 1379 (2000).
- ²⁰K. Mukhopadhyay and S. K. Roy, *Mol. Cryst. Liq. Cryst. Sci. Technol. A* **293**, 111 (1997).
- ²¹J. M. Polson and E. E. Burnell, *Chem. Phys. Lett.* **281**, 207 (1997).
- ²²C. Chiccoli, P. Pasini, and C. Zannoni, *Physica A* **148**, 298 (1988).
- ²³P. A. Lebwohl and G. Lasher, *Phys. Rev. A* **6**, 426 (1972).
- ²⁴W. Maier and A. Saupe, *Z. Naturforsch. A* **14**, 882 (1959).
- ²⁵R. Hashim and S. Romano, *Int. J. Mod. Phys. B* **13**, 3879 (1999).
- ²⁶Z. P. Zhang, M. J. Zuckermann, and O. G. Mouritsen, *Phys. Rev. Lett.* **69**, 2803 (1992).
- ²⁷J. M. Fish and R. L.C. Vink, *Phys. Rev. B* **80**, 014107 (2009).
- ²⁸F. Wang and D. P. Landau, *Phys. Rev. Lett.* **86**, 2050 (Mar 2001).
- ²⁹S. Singh, M. Chopra, and J. J. de Pablo, *Annu. Rev. Chem. Biomol. Eng.* **3**, 369 (2012).
- ³⁰E. B. Kim, R. Faller, Q. Yan, N. L. Abbott, and J. J. de Pablo, *J. Chem. Phys.* **117**, 7781 (2002).
- ³¹P. G. de Gennes and J. Prost, *The Physics of Liquid Crystals*, 2nd ed. (Oxford University Press, New York, 1993).
- ³²N. Rathore, Q. Yan, and J. J. de Pablo, *J. Chem. Phys.* **120**, 5781 (2004).
- ³³M. Doxastakis, Y.-L. Chen, and J. J. de Pablo, *J. Chem. Phys.* **123**, 034901 (2005).
- ³⁴M. Chopra, M. Muller, and J. J. de Pablo, *J. Chem. Phys.* **124**, 134102 (2006).
- ³⁵A. M. Ferrenberg and R. H. Swendsen, *Phys. Rev. Lett.* **61**, 2635 (1988).
- ³⁶J. Lee and J. M. Kosterlitz, *Phys. Rev. Lett.* **65**, 137 (1990).
- ³⁷J. S. Langer, M. Bar-on, and H. M. Diller, *Phys. Rev. A* **11**, 1417 (1975).